Available online at www.sciencedirect.com
ScienceDirect
Journal of the European Ceramic Society 29 (2009) 457–463
www.elsevier.com/locate/jeurceramsoc

Carbon burnout and densification of self-constrained LTCC for fabrication of embedded structures in a multi-layer platform

L.E. Khoong [a,*], Y.M. Tan [a], Y.C. Lam [b]

[a] *Singapore Institute of Manufacturing Technology, 71 Nanyang Drive, Singapore 638075, Singapore*
[b] *Nanyang Technological University, 50 Nanyang Avenue, Singapore 639798, Singapore*

Received 2 June 2008; accepted 20 June 2008
Available online 3 August 2008

Abstract

Carbon burnout and densification of self-constrained low temperature co-fired ceramic (LTCC) are investigated using thermal analysis techniques. Slow heating rates and holding at a temperature higher than initial crystallization temperature of the glass component show evidence of retarding the densification of the self-constrained LTCC. Based on these results, it is proposed that the fabrication of embedded structures in a multi-layer self-constrained LTCC platform could be achieved by controlling carbon burnout with a multi-step co-firing profile, which can ensure complete carbon burnout without affecting the densification of LTCC structures. Using this approach, fabrication of an embedded cavity with dimensions of 10 mm × 10 mm × 0.50 mm in a self-constrained LTCC platform is demonstrated.

Keywords: Sintering; Carbon; Substrate; Sensors; Low temperature co-fired ceramic

1. Introduction

Embedded structures in a multi-layer low temperature co-fired ceramic (LTCC) platform are important for the integration of micro- or meso-systems with complicated features and functionalities. The potential applications include, but are not limited to, sensors, cooling systems, microwave, RF, microfluidics and MEMS devices. Fabrication of embedded structures in a LTCC platform involved steps of structuring, printing, laminating, and co-firing. One of the fabrication challenges is that the embedded structures tend to deform and sag during lamination and/or co-firing.[1–4] This sagging of the embedded structures is due to the non-elastic deformation of the suspended LTCC laminates over the structures subjected to a high lamination pressure (10.3–20.7 MPa) during lamination. During co-firing, LTCC materials undergo debinding and sintering. The glass component softens during sintering. As a result, the suspended LTCC laminates might also deform due to their own body force.

To reduce or to minimize the sagging of the embedded structures to an acceptable level, supporting medium can be employed for embedded structures in a LTCC platform during lamination and/or sintering. Lamination with temporary inserts[5,6] and low pressure lamination with adhesive materials[7–9] were adopted to avoid the deformation of embedded structures during lamination. However, the temporary inserts were removed before co-firing and the adhesive materials were completely burnt out before the sintering of LTCC laminates. Therefore, these two techniques do not provide support for the embedded structures during sintering.

Lead bi-silicate glass was used as a sacrificial material to support the embedded structures during lamination and sintering.[2] However, it was necessary to chemically etched away the glass after sintering and complete removal was difficult. Screen-printed thick film that shrinkage-matched with LTCC was also used as supporting structures to compensate for the deformation induced by the body force during sintering.[2] To support the embedded structures during lamination and sintering, an insert that could be removed after sintering was used.[10] However, a major limitation is that lamination with the insert is not feasible in fabricating enclosed structures.

Multi-layer lamination with fugitive materials was used to support the embedded structures during lamination and/or sintering. These fugitive materials include waxes,[11] polymeric materials,[7,11,12] and carbon materials.[1,2,4,13] Waxes and poly-

* Corresponding author. Tel.: +65 6793 8567; fax: +65 6973 8383.
E-mail address: lekhoong@SIMTech.a-star.edu.sg (L.E. Khoong).

0955-2219/$ – see front matter © 2008 Elsevier Ltd. All rights reserved.
doi:10.1016/j.jeurceramsoc.2008.06.024

meric materials were completely burnt out before the sintering of LTCC laminate, thus no support was provided to the structure during sintering. Controlling of carbon burnout inside the embedded structures provides the opportunity to maintain the carbon as supporting material for the structure during sintering. Since carbon burnout could be suppressed under an inert atmosphere, switching between inert and oxidizing atmospheres was used to control the carbon burnout.[1,2] Another alternative way to control the carbon burnout was by tailoring carbon materials with different carbon particle sizes to ensure complete burnout before pore elimination in LTCC.[4] For the potential of supporting the embedded structures during both lamination and sintering, lamination with carbon material is one of the popular approaches in realizing structures in a LTCC platform.[1,2,4,13] Thus, this investigation focuses on fabrication of embedded structures in self-constrained LTCC platform using carbon material.

To fabricate embedded structure using carbon material, carbon burnout needs to be controlled for (1) avoiding pressure buildup in fragile debound LTCC material before sintering, (2) remaining carbon material as supporting medium for the embedded structures during sintering, and (3) completing carbon burnout before the elimination of open pores in the LTCC material during sintering.

For issue (2), Espinoza-Vallejos et al.[2] controlled carbon burnout by changing the air/nitrogen ratio in the furnace atmosphere during co-firing to maintain the carbon as supporting material for embedded structures during sintering. Our preliminary study showed that the deformation of the suspended self-constrained LTCC laminates over a square cavity with dimensions of 10 mm × 10 mm was less than 100 μm during sintering. Thus, controlling of burnout of the carbon material for it to remain as supporting material during sintering will not be investigated in this paper.

Issues (1) and (3) are the critical issues that have to be addressed for ensuring complete carbon burnout from the LTCC platform with minimum defect. Birol et al.[4] controlled carbon burnout by modifying the carbon material to ensure complete carbon burnout before the elimination of open pores in LTCC. We proposed instead to control carbon burnout by modifying the co-firing profile, which has advantages over control carbon burnout by either modifying the carbon materials[4] or the furnace atmosphere[2]. Effects of modifying the co-firing profile on the carbon burnout and the densification of the self-constrained LTCC were studied using thermal analysis techniques. The study of carbon burnout kinetics shows that carbon burnout could be controlled by changing the heating rate or holding temperature and time. Thermal mechanical analysis (TMA) and differential temperature analysis (DTA) results showed that slow heating rate and holding temperature and time could retard the densification of the self-constrained LTCC due to the induction of crystallization before achieving fully densification. Thus, there is potential to optimize the co-firing profile to control both carbon burnout and the retardation of densification of the self-constrained LTCC.

Based on the studies on carbon burnout and densification behaviors, the fabrication of embedded cavity with dimensions of 10 mm × 10 mm × 0.50 mm was demonstrated using self-constrained LTCC and carbon material. Instead of switching between inert and oxidizing atmospheres[2] or modifying the carbon material,[4] a multi-step co-firing profile was used to control carbon burnout for the fabrication of embedded structures in self-constrained LTCC platform.

2. Methodology

2.1. LTCC and carbon materials

Commercially available self-constrained LTCC tape (HL 2000, Heraues, Germany) and carbon paste (Nano-carbon paste, Harmonics Inc., USA)[14] were used in this study. The self-constrained LTCC tape consists of three sub-layers.[15] The top and bottom sub-layers are made of glass ceramic composite and organic binder. The middle sub-layer is a refractory ceramic layer. The shrinkages in the *x*- and *y*-directions of the tape are constrained when the glass component in the top and bottom sub-layers melt and infiltrate (predominantly in the *z*-direction) into the middle refractory ceramic sub-layer during co-firing. Carbon paste was used as a supporting material for embedded structures during lamination. The carbon paste decomposes and escapes from the LTCC laminates during co-firing.

2.2. Study of carbon burnout

The carbon paste was characterized using TGA equipment (TGA Q500, TA Instruments). The sample size for TGA was about 15 mg. The testing parameters were 1, 5, and 10 °C min^{-1} from 30 to 900 °C in air environment. To study the effect of holding temperature on the carbon burnout, the samples were heated from 30 to 900 °C at 10 °C min^{-1} and the temperatures were held at 700, 750 and 780 °C for 30 min.

The carbon burnout kinetics was studied based on the differential method.[16] The carbon burnout rate was estimated using the rate equation, which is

$$r = \frac{dX}{dt} = k(T)f(X) \quad (1)$$

where r is the carbon burnout rate, $k(T)$ is the temperature-dependent function, $f(X)$ is the composition-dependent term, T is the absolute temperature, and X is the ratio of decomposed carbon weight over the initial carbon weight. $k(T)$ could be expressed using the Arrhenius relationship, which is

$$k(T) = A\ \exp\left(-\frac{E}{RT}\right) \quad (2)$$

where E is the activation energy of the carbon burnout (J/mol), A is the pre-exponential factor (min^{-1}), and R is the universal gas constant (8.314 J/mol K). Assuming a pseudo-first order kinetic relationship,[16] the $f(X)$ can be written as

$$f(X) = (1 - X) \quad (3)$$

Replacing $(1 - X)$ with the weight fraction of residual carbon W and substituting Eqs. (2) and (3) into Eq. (1), the carbon burnout

rate is

$$r = AW \exp\left(-\frac{E}{RT}\right) \tag{4}$$

Taking natural logarithm of both sides, Eq. (4) can be rewritten as

$$\ln\left(\frac{r}{W}\right) = E\left(-\frac{1}{RT}\right) + \ln A \tag{5}$$

Eq. (5) was used to obtain the activation energy E and the pre-exponential constant A for heating rate of 10 °C min^{-1}. From Eq. (1), the residual carbon can be estimated using

$$F(X) = \int_0^X \frac{\mathrm{d}X}{f(X)} = \int_{T_0}^{T_1} \frac{k(T)}{\beta}\,\mathrm{d}T \tag{6}$$

where β is the heating rate. Substituting Eq. (2) into Eq. (6), one obtained

$$F(X) = \int_0^X \frac{\mathrm{d}X}{f(X)} = \int_{T_0}^{T_1} \frac{A}{\beta}\left[\exp\left(-\frac{E}{RT}\right)\right]\mathrm{d}T \tag{7}$$

After determining the activation energy E and the pre-exponential constant A of carbon burnout for a heating rate of 10 °C min^{-1}, Eq. (7) was used to predict the carbon burnout. The Coats–Redfern approximation[17,18] is used to estimate the right hand side of Eq. (7):

$$\int_{T_0}^{T_1} \frac{A}{\beta}\left[\exp\left(-\frac{E}{RT}\right)\right]\mathrm{d}T = \frac{AE}{\beta R}[p(x)]_{x_0}^{x} \tag{8}$$

where

$$p(x) \approx \frac{\mathrm{e}^{-x}}{x^2}\left(1 - \frac{2}{x}\right) \tag{9}$$

$$x = \frac{E}{RT} \tag{10}$$

Expanding the right hand side of Eq. (8) with Eqs. (9) and (10), the residual carbon at temperature T could be estimated as

$$\begin{aligned}&\int_{T_0}^{T_1} \frac{A}{\beta}\left[\exp\left(-\frac{E}{RT}\right)\right]\mathrm{d}T \\ &= \frac{A}{\beta}\left[\frac{RT^2}{E}\left(1 - \frac{2RT}{E}\right)\mathrm{e}^{-(E/RT)}\right. \\ &\left. - \frac{RT_0{}^2}{E}\left(1 - \frac{2RT_0}{E}\right)\mathrm{e}^{-(E/RT_0)}\right]\end{aligned} \tag{11}$$

By substituting the estimated activation energy E and the pre-exponential constant A into Eq. (11), a carbon burnout curve was generated and compared with the TGA curve to confirm the validity of the estimated parameters.

2.3. Study on densification of self-constrained LTCC

The densification of self-constrained LTCC material was studied using thermal analysis techniques. Thermal mechanical analysis (TMA) equipment (TMA 2940, TA instruments) was used to measure the dimensional changes of the material subjected to heating. The samples for TMA were produced by laminating 40 layers of LTCC tapes and pre-cutting into size of 8 mm × 8 mm × 5 mm. The samples were then debound to remove the organic binders in a box furnace. Since the TMA samples were relatively thick (which was 5 mm), slow debinding was required. This slow debinding profile was 30–190 °C at 8 °C/h, 190–500 °C at 0.5 °C min^{-1} and held at 95, 150, and 190 °C for 2 h, respectively. In TMA, the debound samples were heated from 30 to 900 °C at 1, 5, and 10 °C min^{-1}, respectively, in air environment. To study the effects of holding temperature and time on the densification behavior of the self-constrained LTCC, the debound samples were heated from 30 to 900 °C at 10 °C min^{-1} and the temperatures were held at 700 and 750 °C for 30 min and 180 min, respectively.

Crystallization of the self-constrained LTCC material during sintering was also studied using DTA equipment (STA 409C, NETZSCH). The DTA samples were prepared by debinding of the LTCC material to remove the organic binders. The debinding profile was 30–500 °C at 1 °C min^{-1} and held at 500 °C for 1 h. The DTA sample was about 150 mg. The testing parameters were 1, 5, and 10 °C min^{-1} from 30 to 900 °C in air environment.

2.4. Fabrication of embedded structure using carbon material

Mercury instrusion porosimeter (Autopore IV 9500, Micromeritics) was used to measure the open pores to determine the process window for the removal of carbon from the embedded cavity in LTCC laminates. LTCC laminates made of three layers of tapes were first partially sintered at 750 °C in a box furnace prior to porosity measurement. The heating profile was 30–500 °C at 1 °C min^{-1} and 500–750 °C at 8 °C min^{-1}. The LTCC laminates were subsequently cooled down to room temperature. Open pores were measured to study the existence of open pores in the LTCC laminates during sintering.

To fabricate the embedded cavity, four layers of LTCC tapes were first punched with 10 mm × 10 mm cavity. These four LTCC tapes with cavity were combined with another three layers of LTCC tapes to form an open cavity with a depth of 0.50 mm. This cavity was then filled with carbon paste using stencil and subsequently laminated with another three layers of LTCC tapes. As such, embedded cavity with dimensions 10 mm × 10 mm × 0.50 mm was obtained. The LTCC laminate containing embedded cavity filled with carbon paste was then co-fired in box furnace using a modified co-firing profile based on the studies on carbon burnout and densification of self-constrained LTCC. To characterize the deformation of the embedded cavity, stylus profilometer (form Talysurf Series 2, Taylor–Hobson) was used to measure the surface profile of the suspended LTCC over the embedded cavity.

3. Results and discussion

3.1. Burnout behavior of carbon material

Fig. 1(a) shows that the onset of the carbon burnout occurred at higher temperature as the heating rate increased. The onset temperatures of the carbon burnout for heating rate of 1, 5,

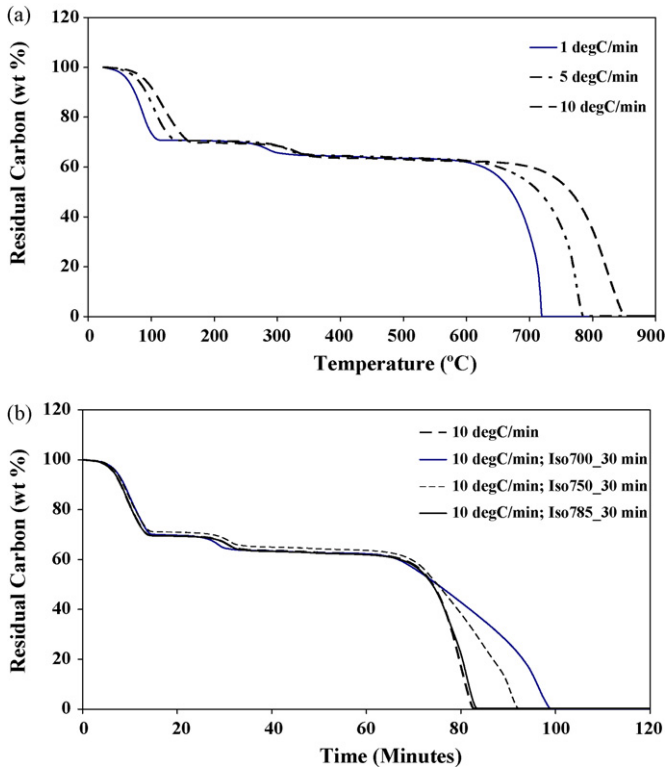

Fig. 1. TGA of carbon burnout in air environment at (a) 1, 5, and 10 °C min^{-1} and (b) 10 °C min^{-1} with holding temperature at 700, 750, and 785 °C for 30 min.

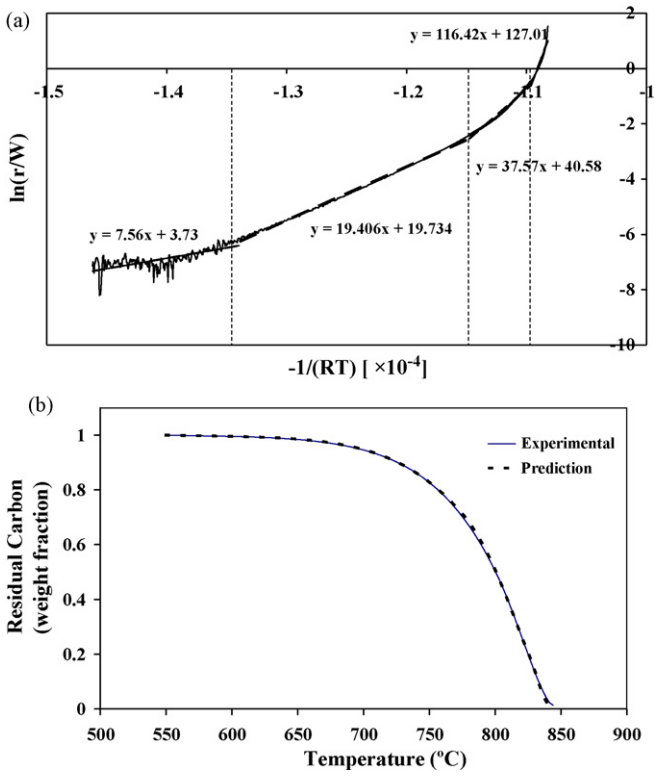

Fig. 2. (a) First-order carbon burnout kinetics plot and (b) comparison of estimated residual carbon with the TGA curve for heating rate of 10 °C min^{-1}.

10 °C min^{-1} were 639, 656, and 729 °C, respectively. The shifting of the onset temperature was because of the shorter time required for the carbon material in achieving higher temperature as heating rates increased.

The effect of holding temperature on the carbon burnout was also studied; see Fig. 1(b). The slopes of the TGA curves indicate the carbon burnout rates. The burnout rates were reduced by holding the temperature at 700 and 750 °C for 30 min. However, the burnout rates were almost similar for the case of without holding or with holding the temperature at 785 °C for 30 min. Thus, temperatures have to be held at suitable points for controlling the carbon burnout rate.

To further understand carbon burnout, first-order carbon burnout kinetics plot was constructed based on Eq. (5); see Fig. 2(a). Based on the assumption of pseudo-first order reaction, carbon underwent four stages of burnout. Activation energies and pre-exponential constants for these four regions of carbon burnout were estimated based on the curve in Fig. 2(a) (see Table 1). The carbon burnout curve was reproduced based on the estimated kinetic parameters using Eq. (11) and was compared with TGA curve to confirm their validity. The good comparison between the predicted and measured carbon burnout shows that this methodology could be used to predict the carbon burnout rate for different heating rate and for different holding temperature and time. This prediction is essential to further optimize the carbon burnout for fabrication of embedded structures with different dimensions and geometries.

Fig. 2(a) and Table 1 show that the activation energies and pre-exponential constants increased with an increase in temperature. The increases in pre-exponential constant and activation energy could affect the onset temperature and the acceleratory portion of the weight loss curves of TGA.[19] As a result, burnout rate increases as temperature increases. The activation energy and pre-exponential constants for 550–625 °C (in Region I) were relatively low, namely 49.7 kJ/mol and 1.20 min^{-1}, respectively. Therefore, there was minimum carbon burnout, which was less than 2 wt.% of total carbon weight, when the carbon was heated at the temperature range in Region I. As temperature increased from 625 to 775 °C (in Region II), the activation energy and pre-exponential constant increased to 194.1 kJ/mol and 3.72×10^8 min^{-1}. About 25 wt.% of total carbon weight was burnt off during this period.

Table 1
Estimated activation energies and pre-exponential constants for four reaction regions of carbon burnout at 10 °C min^{-1}

	Region I	Region II	Region III	Region IV
Temperature range (°C)	550–625	625–775	775–835	>835
Activation energy (kJ/mol)	49.7	194.1	375.7	1220.8
Pre-exponential constant (min^{-1})	1.20	3.72×10^8	4.18×10^{17}	6.91×10^{57}

Significant carbon burnout, which is 60 wt.% burnt off, occurred between 775 and 835 °C (in Region III); see Fig. 2(a) and Table 1. At this temperature range, the activation energy and pre-exponential constant of carbon burnout were estimated to be 375.7 kJ/mol and 4.18×10^{17} min^{-1}. The activation energy and pre-exponential constant could be as high as 1220.8 kJ/mol and 6.91×10^{57} min^{-1} for range above 835 °C (in Region IV). Figs. 1(b) and 2(a) imply that holding the temperature at a point greater than 775 °C (within Regions III and IV) would not slow down the carbon burnout rate as the activation energies and pre-exponential constants were relatively large at this temperature range. Thus, temperature has to be held within 550–775 °C (in Regions I and II) if the suppression of carbon burnout rate is necessary for the embedded structure fabrication.

3.2. Densification of self-constrained LTCC

To establish a modified co-firing profile for carbon burnout without affecting the densification behavior of self-constrained LTCC, effects of co-firing profile on the densification of self-constrained LTCC material were studied. During sintering, shrinkage is dominantly in the *z*-direction, with relatively little shrinkages in the *x*- and *y*-directions (approximately 0.2%).[15] To study the shrinkage in the *z*-direction, dimensional changes (in the *z*-direction) of the self-constrained LTCC material were measured during heating from 30 to 900 °C at a heating rates of 1, 5, and 10 °C min^{-1}, respectively (see Fig. 3(a)). The onset temperature for shrinkage increases from 712 to 740 °C as the heating rate increases from 1 to 10 °C min^{-1}. The shifting in the onset temperature of shrinkage is because of the suppression (or lowering) of the transition temperatures of the glass component with a slower heating rate.

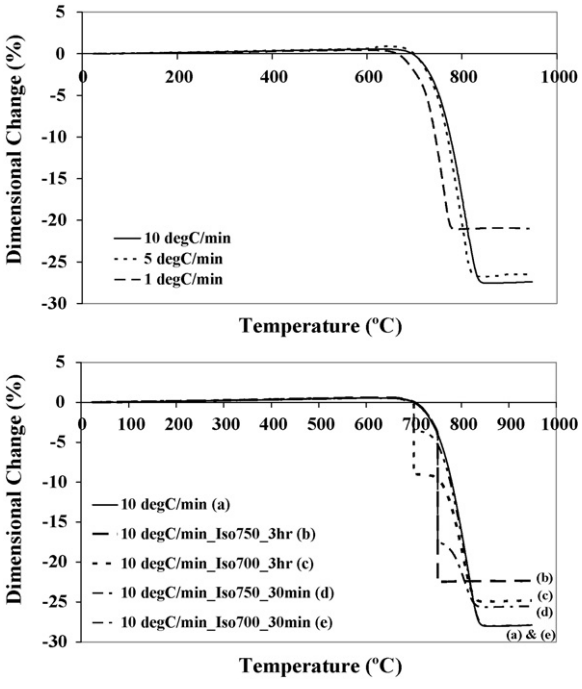

Fig. 3. Dimensional change of self-constrained LTCC in *z*-direction heated in air at (a) 1, 5, and 10 °C min^{-1} and (b) 10 °C min^{-1} with holding temperature at 700 and 750 °C for 30 and 180 min, respectively.

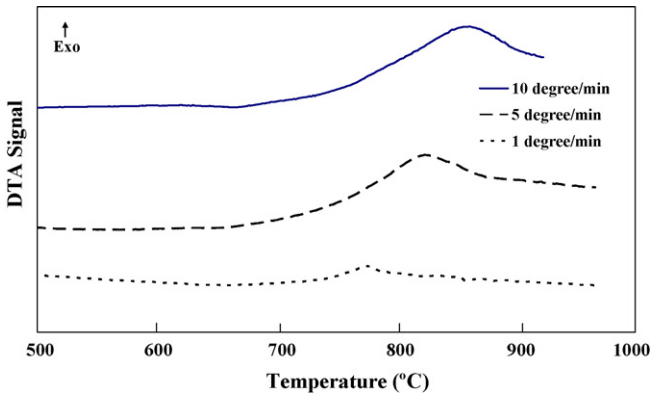

Fig. 4. DTA of self-constrained LTCC for heating rate of 1, 5, and 10 °C min^{-1}.

In addition to affecting the onset temperature of shrinkage, the heating rate affected the degree of shrinkage of self-constrained LTCC. The total shrinkages of self-constrained LTCC heated at 5 and 10 °C min^{-1} were 27–28%; see Fig. 3(a). However, the shrinkage of self-constrained LTCC seemed to be retarded during sintering when heated at 1 °C min^{-1} with a total shrinkage of only 21%. As heating rate decreases, the shrinkages took place over narrower temperature range. The shrinkage of self-constrained LTCC ceased at lower temperature as the heating rates decreases. Shrinkage ceased after 790, 840, and 865 °C for heating rates of 1, 5, and 10 °C min^{-1}, respectively. To further understand the effects of heating rates on the densification of self-constrained LTCC, its phase change was studied using DTA.

Fig. 4 shows the DTA result on self-constrained LTCC. The exothermic crystallization was detected during heating from 30 to 900 °C. The peak crystallization temperatures of the self-constrained LTCC measured for heating rates of 1, 5, and 10 °C min^{-1} were 780, 830, and 860 °C, respectively. Combination of Figs. 3(a) and 4 indicates that the crystallization of glass component could have retarded the shrinkage or densification of the self-constrained LTCC. During crystallization, the viscosity of the glass component increases to near infinity.[20] As a result, the diffusion of glass component from the top and bottom sublayers into the inner refractory ceramic sub-layer was inhibited and hence retarded the densification.

The effects of holding temperature and time on the shrinkage of self-constrained LTCC for a heating rate of 10 °C min^{-1} were also studied (see Fig. 3(b)). Comparing curves (d) and (e) in Fig. 3(b), there was more shrinkage (which was 17%) during the holding of temperature at 750 °C for 30 min as compared to that of temperature holding at 700 °C for 30 min (which was 4%). This result indicates that holding the temperature after the onset temperature of shrinkage (which was 705 °C) could not significantly prevent the material from shrinking.

The densification of the self-constrained LTCC was not affected after holding the temperature at 700 °C for 30 min. The total shrinkage remained similar to that of heated at 10 °C min^{-1} without holding the temperature; see curves (a) and (e) in Fig. 3(b). However, the total shrinkage reduced to 26 and 22%

for the case of holding the temperature at 750 °C for 30 min and 3 h, respectively; see curves (a), (b), and (d) in Fig. 3(b). The decrease in shrinkage could be due to the occurrence of crystallization at 740 °C, which could retard the densification (see Fig. 4). Comparing curves (c) and (d) in Fig. 3(b), similar total shrinkage was observed for holding the temperature and time at 700 °C for 3 h and 750 °C for 30 min. This implies that holding the temperature at 700 °C for a relatively long period might induce crystallization that subsequently retarded densification. Based on these results, a preliminary guideline was established in modifying the co-firing profile for carbon burnout for the fabrication of embedded structures.

3.3. Fabrication of embedded structure using carbon materials

Instead of controlling carbon burnout by modifying carbon particle size,[4] TGA results indicate that carbon burnout could be controlled by changing heating rates and/or holding temperature and time (Fig. 1(a) and (b)).

For issue (1), which is to avoid pressure buildup in the fragile debound LTCC material, burnout rate has to be suppressed before or at the early stage of sintering. Based on the TGA analysis, carbon burnout could be suppressed by holding the temperature within 625–775 °C in Region II (see Fig. 2(a)). At this temperature range, the activation energy and pre-exponential constant of the carbon burnout are relatively low (which are 194.1 kJ/mol and 3.72×10^8 min^{-1}).

To resolve issue (3), which is for complete carbon burnout before the elimination of open pores, the open pore elimination temperature for the self-constrained LTCC has to be determined. Birol et al.[4] estimated that the closure of open pores in LTCC material (which is DuPont 951-C2) occurred at 50% of total shrinkage. TMA result shows that the densification of self-constrained LTCC occurred between 700 and 840 °C with 50% of total shrinkage achieved at 765 °C (see Fig. 3(a)). Based on this TMA result, the open pore measurements were conducted on partially sintered self-constrained LTCC laminates at 750 °C using mercury intrusion porosimeter. The open porosity for the partially sintered self-constrained LTCC laminates made of three layers of tapes was measured to be 42.5 ± 1.0%. Since the existence of the open pores were observed in the partially sintered self-constrained LTCC (at 750 °C), it is possible to completely removed the carbon material before 750–760 °C from the embedded structure enclosed with relatively thin suspended LTCC laminates of three layers or less.

In modifying the co-firing profile for carbon burnout, the effects of changing the co-firing profile on the densification of the self-constrained LTCC have to be considered. Slow heating rates and overly long period of temperature holding could retard the densification of the material (Fig. 3(b)). To suppress the carbon burnout or to ensure complete burnout, the temperature should be held at the points lower than the initial crystallization temperature of the self-constrained LTCC (Figs. 3(b) and 4). We also found that holding the temperature above the initial crystallization temperature (which is 740 °C) for a relatively long period should be avoided.

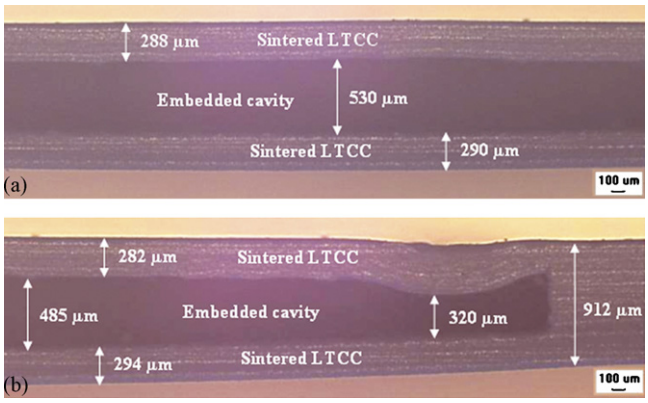

Fig. 5. Cross-section of (a) the center portion and (b) the corner portion of an embedded cavity fabricated using carbon material with a modified co-firing profile.

Based on these understandings on the carbon burnout and densification behaviors, we employed a multi-step co-firing profile to control the carbon burnout. The LTCC laminate containing an embedded cavity filled with carbon paste was first heated from 30 to 450 °C at 1 °C min^{-1} to remove the organic binders. At the early stage of carbon burnout, less aggressive carbon burnout rate was preferred since a LTCC laminate was fragile after debinding and before sintering. Thus, the LTCC laminate was further heated from 450 to 700 °C at 8 °C min^{-1} and held at 700 °C for 30 min to suppress the carbon burnout rate. At the later stage of the carbon burnout, the LTCC laminate was heated from 700 to 750 °C at 8 °C min^{-1} and held again at 750 °C for 15 min to ensure the complete carbon burnout before the open pores in the LTCC laminate were completely closed. Subsequently, the furnace temperature was increased from 750 to 875 °C at 8 °C min^{-1} and held at 875 °C for 15 min to fully densify the LTCC laminate. Embedded cavity with dimensions of 10 mm × 10 mm × 0.50 mm was realized in the self-constrained LTCC platform as shown in Fig. 5(a) and (b). The depth of the embedded cavity ranges from 485 to 530 μm along the width of the cavity (excluding the edge). The deformation of the embedded cavity was minimized. Instead of sagging, the surface profile of the suspended LTCC over the embedded cavity was found swelling; see Fig. 5(a). The edges of the embedded cavity could be improved by optimizing the filling technique of carbon paste into structures; see Fig. 5(b). Comparing to the current techniques of switching gases[2] and modifying carbon material,[4] this technique of using multi-step carbon burnout process and self-constrained LTCC is a more convenient and low cost way to control carbon burnout for the realization of embedded structures in LTCC -based platform.

4. Conclusions

The controlling of carbon burnout is critical to ensure complete carbon burnout with minimum defect for the fabrication of embedded structures in self-constrained LTCC platform. The control of carbon burnout was demonstrated by modifying the co-firing profile instead of switching gases or modifying the car-

bon material. To suppress the carbon burnout rate, temperature has to be held at temperature range in which the activation energy and pre-exponential constant of the carbon burnout are relatively low (which are 194.0 kJ/mol and 3.72×10^8 min^{-1}). The TMA and DTA results revealed that a slow heating rate and holding the temperature after the occurrence of initial crystallization of the glass component (which is 740 °C) could retard the densification of the material during sintering. Thus, the co-firing profile has to be modified accordingly for complete carbon burnout. Studies of the carbon burnout and densification behaviors of self-constrained LTCC during sintering provided a guideline for the optimization of the co-firing profile for carbon burnout in the realization of embedded structures in LTCC-based platform.

Acknowledgments

The authors would like to acknowledge SIMTech, Agency for Science, Technology and Research (A*STAR), Singapore and NTU for project funding and support.

References

1. Bau, H., Ananthasuresh, S., Santiago-Aviles, J. J., Zhong, J., Kim, M., Yi, M. *et al.*, Ceramic tape based meso systems technology. In *Proceedings of the ASME International Mechanical Engineering Congress and Exposition*, 1988, pp. 491–498.
2. Espinoza-Vallejos, P., Zhong, J.-H., Gongora-Rubio, M. R., Sola-laguna, L. and Santiago-Aviles, J. J., Meso (Intermediate)-scale electromechanical systems for the measurement and control of sagging in LTCC structures. *Mater. Res. Soc. Symp. Proc.*, 1998, **518**, 3–79.
3. Gongora-Rubio, M. R., Espinoza-Vallejos, P., Sola-Laguna, L. and Santiago-Aviles, J. J., Overview of low temperature co-fired ceramics tape technology for meso-system technology (MsST). *Sensors Actuat. A Phys.*, 2001, **89**, 222–241.
4. Birol, H., Maeder, T. and Ryser, P., Processing of graphite-based sacrificial layer for microfabrication of low temperature co-fired ceramics (LTCC). *Sensors Actuat. A Phys.*, 2006, **130–131**, 560–567.
5. Bauer, R., Luniak, M., Rebenklau, L., Wolter, K.-J. and Sauer, W., Realization of LTCC-multilayer with special cavity applications. In *In 30th International Symposium on Microelectronics (ISHM'97)*, 1997, pp. 659–664.
6. Miehls, D. J., Martin, F. J., Pond, R. G., and Fleischner, P. S. Method of fabricating a multilayer electrical circuit. US Patent 5249355 (5 October 1993).
7. Roosen, A., New lamination technique to join ceramic green tapes for the manufacturing of multilayer devices. *J. Eur. Ceram. Soc.*, 2001, **21**, 1993–1996.
8. Jones, W. K., Liu, Y. and Gao, M., Micro heat pipes in low temperature co-fired ceramic (LTCC) substrates. *IEEE Trans. Comp. Packag. Technol.*, 2003, **26**, 110–115.
9. Burdon, J. W., Huang, R. -F., Wilcox, D., and Naclerio, N. J., Method for fabricating a multilayered structure and the structures formed by the method. US Patent 6592696 (15 July 2003).
10. Cawley, J. D., Heuer, A. H., and Newman, W. S., Method of constructing three dimensional bodies from lamination. US Patent 5777833 (14 July 1998).
11. Trickett, E. A. and Assmus, R. C., Ceramic monolithic structure having an internal cavity contained therein and a method of preparing the same. US Patent 4806295 (21 February 1989).
12. Alexander, J. H., Method of making ceramic article with cavity using LTCC tape. US Patent 5601673 (11 February 1997).
13. Peterson, K. A., Patel, K. D., Ho, C. K., Rohde, S. B., Nordquist, C. D., Walker, C. A. *et al.*, Novel microsystem applications with new techniques in low-temperature co-fired ceramics. *Int. J. Appl. Ceram. Technol.*, 2005, **2**, 345–363.
14. Technical note on high purity carbon tape and paste. Harmonics, Inc. http://www.harmonicsmaterials.com/.
15. Rabe, T., Schiller, W. A., Hochheimer, T., Modes, C. and Kipka, A., Zero shrinkage of LTCC by self-constrained sintering. *Int. J. Appl. Ceram. Technol.*, 2005, **2**, 374–382.
16. Chan, J. H. and Balke, S. T., The thermal degradation kinetics of polypropylene. Part II. Thermogravimetric analyses. *Polym. Degrad. Stabil.*, 1997, **57**, 135–149.
17. Coats, A. W. and Redfern, J. P., Kinetic parameters from thermogravimetric data. *Nature*, 1964, **201**, 68–69.
18. Doyle, C. D., Series approximations to the equation of thermogravimetric data. *Nature*, 1965, **207**, 290–291.
19. Brown, M. E., *Introduction to Thermal Analysis: Techniques and Applications*. Chapman and Hall, New York, 1988, pp. 144–50.
20. Lo, C. L., Duh, J. G. and Chiou, B. S., Low temperature sintering and crystallization behavior of low loss anorthite-based glass-ceramics. *J. Mater. Sci.*, 2003, **38**, 693–698.